Applied Surface Science 255 (2009) 5471–5475

Contents lists available at ScienceDirect

Applied Surface Science

journal homepage: www.elsevier.com/locate/apsusc

Micro-patterning for polymer electrolyte fuel cells: Single pulse laser ablation of aluminum films from glassy carbon

Bernhard C. Seyfang [a], Romain Fardel [b], Thomas Lippert [a,*], Guenther G. Scherer [a], Alexander Wokaun [a]

[a] Paul Scherrer Institut, General Energy Research Department, 5232 Villigen PSI, Switzerland
[b] Empa, Swiss Federal Laboratories for Materials Testing and Research, Laboratory for Functional Polymers, Überlandstrasse 129, 8600 Dübendorf, Switzerland

ARTICLE INFO

Article history:
Available online 8 August 2008

Keywords:
Laser ablation
Aluminum film
Glassy carbon
ns-Shadowgraphy
Micropolymer electrolyte fuel cell

ABSTRACT

Microfuel cells are a possible replacement for batteries as energy sources in portable devices. At PSI a micropolymer electrolyte fuel cell was developed, whose flow fields consist of micro-structured glassy carbon plates. Micro-structuring of glassy carbon is carried out in a multi-step process. A sputtered aluminum mask is selectively removed by single pulse laser ablation from glassy carbon thereby defining micro-channels subsequently etched by reactive ion etching.

A pulsed XeCl excimer laser (308 nm) is used for the single pulse patterning of a metal mask on the glassy carbon. The influence of the excimer laser typical pulse to pulse energy fluctuations on the micro-structuring process must be known to minimize defects during RIE etching of the micro-channels. To obtain a better understanding of the processes occurring during ablation, ns-shadowgraphy was performed. The formation of a shockwave was observed, followed by a similar but much slower perturbation, and the subsequent release of fragments. The calculated velocities can be correlated with the energy release during ablation. The post-ablation examination of the samples by profilometry, optical microscopy, SEM and EDX is used to measure the amount of removed material, the quality of the aluminum mask edges and aluminum residues on the glassy carbon surface. Such criteria allow us to classify the laser irradiation as a function of laser fluence: no ablation, partial ablation, complete ablation, and over-ablation.

1. Introduction

Microfuel cells are suggested as possible alternatives to Lithium Ion batteries as energy source in hand-held devices, such as laptops and cell phones. Advantages are the easy recharging as well as the high energy density. Several concepts have been presented by industry and research for different types of fuel cells [1,2].

At PSI a micropolymer electrolyte fuel cell (PEFC) was developed which consists of three main parts, i.e. the two micro-structured glassy carbon based flow fields and a catalyst-coated membrane sandwiched between those two glassy carbon plates. During fuel cell tests, a power density of 395 mW/cm^2 (at 500 mV cell voltage, cell temperature = 50 °C, stoichiometry(H_2) = 1.7 @ 1 A/cm^2, stoichiometry(O_2) = 2.1 @ 1 A/cm^2, 80% R.H. of the gases) [3] could be obtained.

The micro-patterning of glassy carbon is a sequence of polishing, followed by magnetron sputtering of an aluminum mask onto the glassy carbon surface. The flow field structure is written by laser ablation into this mask. Finally, the micro-channels are formed by oxidative removal of the glassy carbon material from the unmasked areas by reactive ion etching (RIE) using oxygen as process gas. The aluminum of the mask is passivated and remains stable during RIE [4–6].

A crucial step in the patterning of the microchannels is the single pulse laser ablation of the aluminum mask. A pulsed 308 nm XeCl laser is employed to remove the aluminum from the area, where micro-channels will be formed in the subsequent etching step. Hence, it is important to understand the mechanisms of single pulse laser ablation while removing the Al-layer. The aluminum has to be removed selectively whereas the remaining Al-mask should not be damaged.

The method of ns-shadowgraphy has been utilized to observe the processes (e.g. plasma formation), products (fragments), and shockwaves during laser ablation [7]. The latter observation can be used to obtain information about the energy released during ablation.

Several publications deal with laser ablation of aluminum, also in combination with shadowgraphy [8–13]. Jeong et al. [8]

* Corresponding author. Tel.: +41 56 310 4076; fax: +41 56 310 4412.
E-mail address: thomas.lippert@psi.ch (T. Lippert).

0169-4332/$ – see front matter © 2008 Elsevier B.V. All rights reserved.
doi:10.1016/j.apsusc.2008.07.189

investigated the laser ablation processes from bulk aluminum by ns-shadowgraphy. Employing a 248 nm excimer laser they observed a shockwave as well as the formation of a vapor plume. The authors also discuss the correlation of the threshold laser fluence and the reflectivity of aluminum and give a threshold value of ~8 J/cm^2 for a reflectivity of 0.92 [9]. The reflectivity was already given by [10] and counts also for an irradiation wavelength of 308 nm. First investigations on the laser ablation of aluminum films using a XeCl excimer laser were carried out by Andrew et al. [11]. For aluminum they propose that melting and explosive mechanisms occurring on the interface are responsible for the film removal. Schultze and Wagner [12] describe the 'blow-off' of aluminum films with a thickness of 0.8 μm from a transparent substrate by irradiation through the substrate, employing a Nd:YAG laser. The assumed mechanism again is based on melting that is followed by vaporization at the substrate–metal interface. The vapor pressure then results in bubble formation and finally removes the liquid aluminum from the surface. Dyer et al. [13] investigated the ablation of aluminum films (80 and 300 μm) from PET and α-Si:H. They indicate the thermal diffusion profiles in the film-substrate combination as detrimental for sufficient film removal by a 'blow-off' mechanism. The ablated aluminum forms droplets due to Rayleigh-Taylor instabilities, caused by acceleration of the fluid-state film.

Due to a different substrate material and different film dimensions, the cases treated in the literature [8–13] are not directly applicable to our present experimental configuration. Therefore a detailed analysis of the single pulse laser process and the samples after the partial removal of the aluminum is required.

2. Experimental

The glassy carbon samples (Sigradur G, HTW, D-Thierhaupten, 12 mm × 12 mm × 1 mm) were polished for 2 min in an aqueous suspension of Al_2O_3 (Buehler, 3 μm) on a textile clothe (Buehler), followed by a 1 min ultrasonic treatment in ultra-pure water (18 MΩ cm) and dry-blowing with nitrogen. Aluminum layers with a thickness of 280, 570 and 850 nm were deposited by magnetron sputtering. One part of the glassy carbon sample was covered during sputtering allowing to determine the thickness of the aluminum layers using a Profilometer (Veeco DekTak 8).

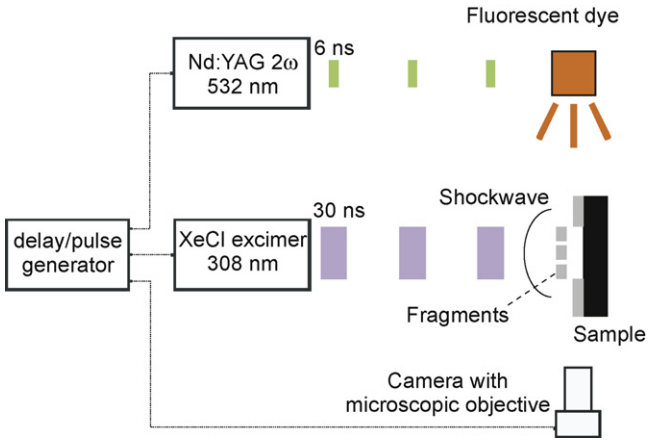

Fig. 1. Scheme of the ns-shadowgraphy arrangement. The delay generator controls the time difference between pump and probe laser to visualize the processes happening close to the surface of the sample at different time delays.

The samples were irradiated with a 308 nm XeCl excimer laser (pulse length 30 ns) to write the pattern into the Al-layer. The beam passes through a 2.7 mm × 2.7 mm aperture and is focused by a lens to a spot size of 135 μm × 135 μm. Each pulse was directed onto a new sample position. The ablation plume was illuminated by a fluorescent dye pumped with a Nd:YAG laser at a wavelength of 532 nm (2nd harmonic). A pulse/delay generator controlled the delay between the pump and the probe laser. To record the shadowgraphy photographs, a camera with zoom objective was positioned in-line with the sample and the dye (Fig. 1).

Typical observations made by ns-shadowgraphy during the single pulse ablation process are shown in Fig. 2. A shockwave is formed directly after irradiation. The shockwave is visible in air due to a layer of compressed air with a different refractive index. After several hundred nanoseconds, a second distortion becomes visible, which resembles a shockwave but moves much slower. Finally, fragments of the ablated Al-film can be observed.

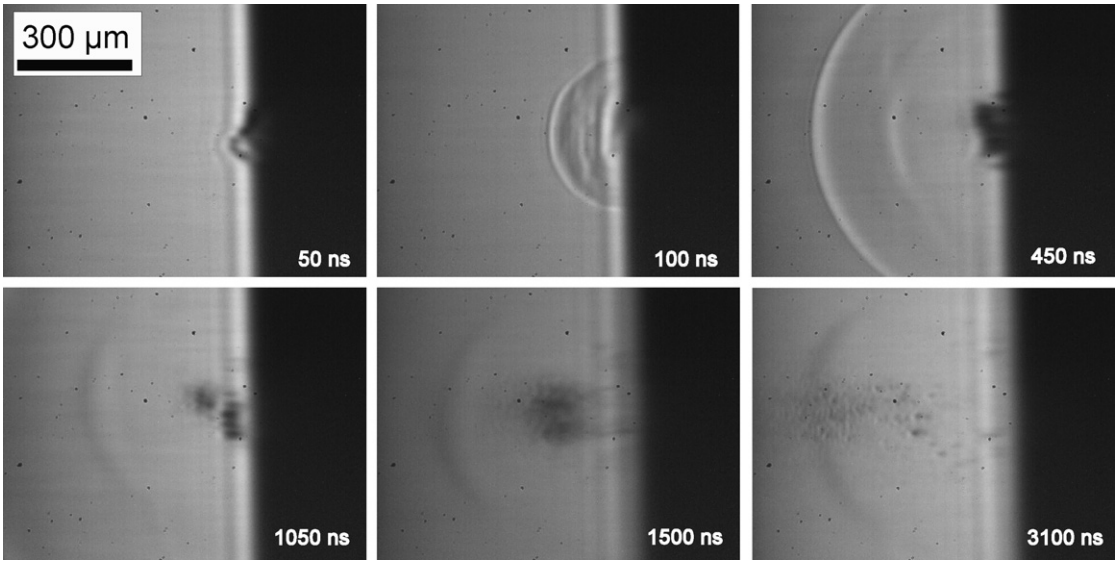

Fig. 2. Single photographs recorded during ablation of a sample with 570-nm thick Al-layer at a laser fluence of 3.0 J/cm^2. Time delays are given for each picture.

The relation of the distance the shockwave traveled and time delay can be fitted by Eq. (1). It is based on Eq. (2), as given by Jeong et al. [8].

$$r_{sw}(t) = At^{\alpha} \tag{1}$$

$$r_{sw} = \left(\frac{E_0}{\alpha \rho_{\infty}}\right)^{1/(n+2)} t(r_{sw})^{2/(2+n)} \tag{2}$$

r_{sw} represents the distance of the shockwave from the substrate, E_0 is the blast wave energy, α is a constant, ρ_{∞} is the density of the undisturbed ambient gas, and t is the time delay. The analysis of dr_{sw}/dt yields then the propagation velocity of the shockwave.

An Alcatel GIR300 etching chamber with glass-covered 6 in. electrodes was employed for the reactive ion etching. The samples remained in the plasma for 15 min under an O_2 atmosphere of 8 Pa and an RF power of 200 W.

3. Results

3.1. Laser fluence effects

In Fig. 3, four different categories of laser induced interaction can be determined from the pictures showing the samples after ablation. The diagram representing the shockwave velocity as a function of laser fluence is sectioned according to those observations.

For fluences below 1.3 J/cm^2, no significant amount of aluminum is removed. A slightly higher shockwave speed is observed than for slightly higher fluences, probably due the fact that no energy is consumed for the vaporization of aluminum.

Above 1.3 J/cm^2, aluminum removal in significant amounts is observed, but only parts of the aluminum mask are removed from the irradiated area. In areas where the Al is removed, the complete layer is ablated. The SEM micrograph recorded from this sample reveals that the edge of the aluminum mask is not well defined. A part of the mask still covers the delaminated glassy carbon area. The glassy carbon surface looks on the other hand, undamaged and is free from aluminum residues, as EDX measurements reveal.

At higher fluences (~3.0 J/cm^2), the aluminum is removed completely from the irradiated area and a minor ablation of glassy carbon is observed. A steep increase in the shockwave velocity is visible compared to the values given for lower fluences. Additionally, the second distortion following the shockwave is more pronounced in the shadowgraphy micrographs. The amount of aluminum residues on the surface increases. EDX measurements reveal a relative aluminum to carbon signal of 0.4%. The edge of the removed Al layer looks relatively sharp, although a slight overlapping part of the aluminum mask is still visible.

When the fluence is increased above ~3.0 J/cm^2, so-called over-ablation is observed. The shockwave velocity increases further and at 5.4 J/cm^2 a plasma is formed. The plasma absorbs parts of the laser light, which explains the reduced increase of the shockwave velocity compared to the trend shown for lower fluences [14,15]. The photographs suggest a large amount of aluminum still being present on the glassy carbon surface. Next to the damaged edge of the aluminum mask, a several microns wide region is visible, that was not irradiated and where no aluminum is deposited. Inside the irradiated area large droplets of molten and re-solidified aluminum are observed on the surface. Quantification by EDX reveals a strongly increasing amount of aluminum compared to ablation at lower fluences (1.3% for 3.5 J/cm^2, 4.8% for 5.4 J/cm^2, respectively).

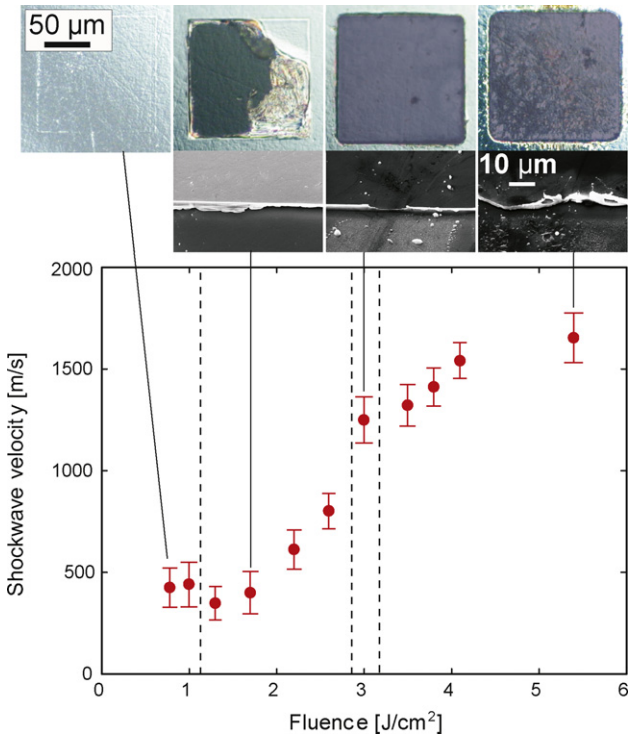

Fig. 3. Velocity of the shockwave, 100 ns after irradiation, plotted vs. laser fluence for laser ablation of a 570 nm thick aluminum film from glassy carbon. The pictures in the upper row represent the ablated spots at the indicated laser fluences under an optical microscope. The SEM micrographs in the lower line show the edges of the aluminum mask after ablation.

3.2. Influence of the Al-film thickness

The influence of the aluminum layer thickness on the ablation for a fixed laser fluence is presented in Fig. 4.

A fluence of 3.0 J/cm^2 is not high enough to remove a 850 nm thick film completely from the irradiated area. The remaining mask reveals again bubbles, which seem to be more defined probably due to a mechanically more stable film, than shown for a thinner film at lower fluences. For the 280 nm thick film, irradiation with a

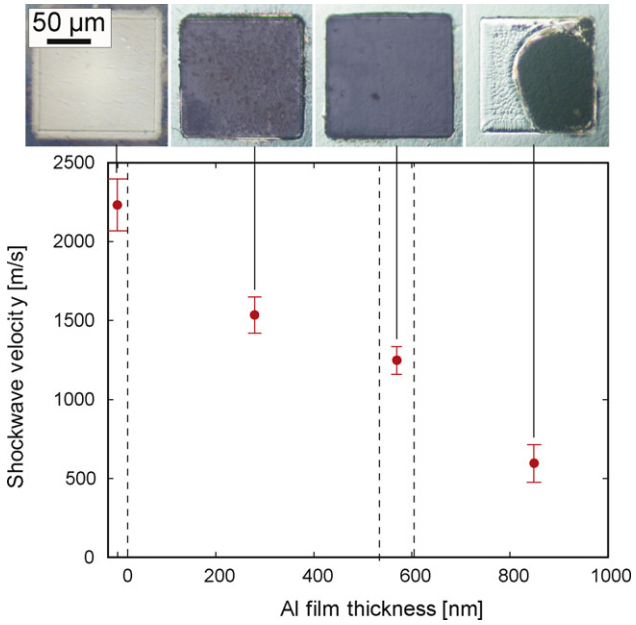

Fig. 4. Velocity of the first shockwave, 100 ns after irradiation, plotted vs. the thickness of the aluminum layer, at a fluence of 3.0 J/cm^2. The photographs represent the samples after ablation.

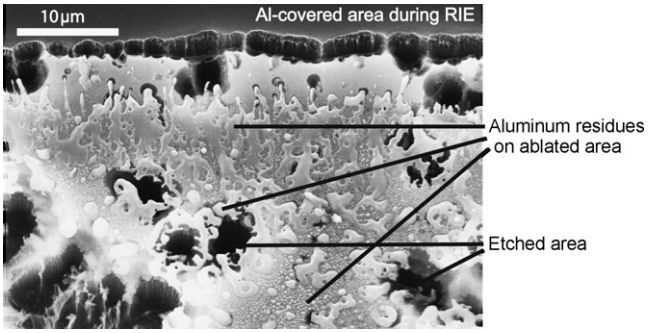

Fig. 5. SEM micrograph showing a sample where the aluminum mask was ablated at a fluence of 5.4 J/cm^2, followed by a 15 min treatment under O_2-plasma.

fluence of 3.0 J/cm^2 results in complete removal of the mask, but also in severe damage of the edges and a high amount of aluminum remaining on the glassy carbon. The shockwave velocity shows also a steep increase, as soon as complete ablation is taking place.

On a sample without Al-film, bulk glassy carbon is ablated at a fluence of 3.0 J/cm^2. A high shockwave velocity is observed here.

3.3. Reactive ion etching after laser ablation at high fluence (5.4 J/cm^2)

After laser ablation reactive ion etching is used to remove the unmasked glassy carbon and to form micro-channels. The consequences of 'over-ablation' are significant as shown in Fig. 5. Close to the edge, where no remaining aluminum is present, a vertical RIE etch rate similar to values reported by Kuhnke et al. [5] can be observed. Due to the damaged edge of the aluminum mask, no straight glassy carbon edges are formed during reactive ion etching. Another influence is observed in areas where molten aluminum remains on the glassy carbon surface. The aluminum is passivated in the oxygen plasma and hence not removed during the RIE process, while the uncovered glassy carbon is oxidized and removed. The results are holes and remaining glassy carbon areas which is not desired when well-defined micro-structures are needed.

4. Discussion

In comparison to the data given by Jeong et al. [9], the ablation threshold is significantly lower for our thin film system than for bulk aluminum. von Allmen [10] gives an absorption coefficient of $\sim 10^6$ cm^{-1} for aluminum at 308 nm, resulting in a light penetration depth of 10 nm. Heat conduction can be assumed as the main reason for energy transfer within the sample. The pronounced difference of heat conductivity for aluminum (237 W m^{-1} K^{-1}) and for Sigradur G (6.3 W m^{-1} K^{-1}) suggests that heat accumulation at the Al–GC interface is responsible for the delamination of the aluminum film. Dyer et al. [13] report about such an effect already for a lower difference in heat conductivity, but thinner aluminum films. In the case of partial ablation, the area still covered with aluminum reveals the formation of bubbles, similar to observations made by Schultze and Wagner [12]. This observation supports the hypothesis about the formation of a gaseous components at the glassy carbon/aluminum interface. The expanding gases cause ejection of the complete film, an effect that has also been named as buckling effect.

For very high fluences, the perturbation of the liquefied film as reported by Dyer et al. [13] occur already close to the GC–Al interface. In combination with severe damage of the glassy carbon substrate it could be responsible for the deposition of large aluminum amounts on the glassy carbon surface. Plasma formation cannot be the main reason for the aluminum deposition because it is only observed for fluences $\geq$5.4 J/cm^2.

When complete takes place, a steep increase in the shockwave velocity as a function of fluence reveals a substantial change in the ablation regime. Additionally, the second perturbation is more pronounced. Both effects could be due to an increased energy release possibly caused by exothermal decomposition of carbon or by thermal expansion of gas trapped in micropores existing in the glassy carbon. Similar to our observation, a second perturbation has also been described by Bennett et al. [16] during laser ablation and ns-shadowgraphy of a photosensitive polymer film. The appearance of a second blast wave was assigned to a secondary or delayed reaction taking place, causing a delayed vaporization of products. The relatively high shockwave velocity obtained for ablation of bulk glassy carbon in comparison to Al-films supports the hypothesis that either gas release from micropores or thermal decomposition contributes to the energy release. Nevertheless, a reflection of the first shockwave on the backside of the glassy carbon sample cannot be excluded completely, as estimates of the shockwave reflection reveal a similar timescale.

The amount of aluminum present on the surface increases strongly if the fluence is $>$3.0 J/cm^2. This limits the optimum processing window in terms of fluence. For the applied excimer laser pulse to pulse fluctuations in the range of $\pm$18% are observed. This suggests that an optimum processing window has to be selected carefully. ns-Shadowgraphy can be applied to determine the correct fluence by the energy release increase appearing as soon as complete ablation is reached.

5. Conclusion

Our results suggest that laser irradiation of aluminum films on glassy carbon substrates can be divided into four different classes: no ablation, partial ablation, complete ablation and over-ablation.

The parameters that determine this classification are laser fluence and the thickness of the aluminum film. The ratio of uncovered to irradiated glassy carbon, the amount of residual aluminum on the glassy carbon surface, and the shape of the aluminum mask edges are characteristics for the different categories. The velocity of the observed shockwave and fragments show a steep increase and identify the transition from partial ablation to complete ablation. The formation of bubbles in the layer at lower fluence as well as the aluminum deposition on the glassy carbon surface at higher fluence, indicate that aluminum vaporization at the interface plays an important role during the removal of the Al layer from the carbon substrate.

For successful micro-structuring, it is important that the amount of remaining aluminum on the glassy carbon surface is as small as possible. Having said that, the aluminum mask has to be removed completely from the irradiated area. It is important to define the laser fluence for ablation as precise as possible. If this is not the case, typical energy fluctuations of the excimer laser can have a direct impact on the following micro-structuring step, i.e. badly defined micro-structures resulting in a reduced power output of the microfuel cell.

Acknowledgements

The contributions of Fredy Glaus, Michael Horisberger and Hendrik Schulenburg as well as financial support from Paul Scherrer Institut and from the Swiss National Science Foundation are gratefully acknowledged.

References

[1] N.-T. Nguyen, S.H. Chan, J. Micromech. Microeng. 16 (2006) R1.
[2] J.D. Morse, Int. J. Energy Res. 31 (2007) 576.

[3] B.C. Seyfang, M. Kuhnke, T. Lippert, G.G. Scherer, A. Wokaun, Electrochem. Commun. 9 (2007) 1958.
[4] M. Kuhnke, T. Lippert, E. Ortelli, G.G. Scherer, A. Wokaun, Thin Solid Films 453–454 (2004) 36.
[5] M. Kuhnke, T. Lippert, G.G. Scherer, A. Wokaun, Surf. Coat. Technol. 200 (2005) 730.
[6] M. Kuhnke, G. Dumitru, T. Lippert, E. Ortelli, G.G. Scherer, A. Wokaun, J. Laser Micro/Nanoeng. 1 (2006) 67.
[7] M. Hauer, D.J. Funk, T. Lippert, A. Wokaun, Opt. Lasers Eng. 43 (2005) 545.
[8] S.H. Jeong, R. Greif, R.E. Russo, J. Phys. D: Appl. Phys. 32 (1999) 2578.
[9] S.H. Jeong, R. Greif, R.E. Russo, Appl. Surf. Sci. 127–129 (1998) 177.
[10] M. von Allmen, Laser Beam Interactions with Materials, Springer, Berlin, 1987.
[11] J.E. Andrew, P.E. Dyer, R.D. Greenough, P.H. Key, Appl. Phys. Lett. 43 (1983) 1076.
[12] V. Schultze, M. Wagner, Appl. Phys. A 53 (1991) 241.
[13] P.E. Dyer, D.M. Karnakis, P.H. Key, D. Sands, Appl. Surf. Sci. 109–110 (1997) 168.
[14] F. Fuso, L.N. Vyacheslavov, G. Lorenzi, M. Allegrini, E. Arimondo, Appl. Surf. Sci. 96–98 (1996) 181.
[15] S. Amoruso, M. Armenante, V. Berardi, R. Bruzzese, N. Spinelli, Appl. Phys. A 65 (1997) 265.
[16] L.S. Bennett, T. Lippert, H. Furutani, H. Fukumura, H. Masuhara, Appl. Phys. A 63 (1996) 327.